The Crystal Lattice of *Paramecium* Trichocysts before and after Exocytosis by X-ray Diffraction and Freeze-Fracture Electron Microscopy

Linda Sperling, Annette Tardieu, and Tadeusz Gulik-Krzywicki

Centre de Génétique Moléculaire, Centre National de la Recherche Scientifique, 91190 Gif-Sur-Yvette, France

Abstract. *Paramecium* trichocysts are unusual secretory organelles in that: (*a*) their crystalline contents are built up from a family of low molecular mass acidic proteins; (*b*) they have a precise, genetically determined shape; and (*c*) the crystalline trichocyst contents expand rapidly upon exocytosis to give a second, extracellular form which is also an ordered array. We report here the first step of our study of trichocyst structure. We have used a combination of x-ray powder diffraction, freeze-etching, and freeze-fracture electron microscopy of isolated, untreated trichocysts, and density measurements to show that trichocyst contents are indeed protein crystals and to determine the elementary unit cell of both the compact intracellular and the extended extracellular form.

CELLS package the proteins they export in a variety of physical states. Although the basic mechanisms involved in the synthesis, concentration, storage, and secretion of these proteins are essentially the same in all instances (Palade, 1975), the contents of a secretory granule may be a solution of macromolecules, a charge-neutralized precipitate that is either soluble or insoluble once it has left the cell, or a crystal (Poisner and Trifaró, 1982).

The trichocysts of *Paramecium*, like other protozoan "extrusosomes" (Hausmann, 1978), are secretory organelles in which proteins are packaged with crystalline organization. Unlike any known metazoan secretory granule, the trichocyst contents not only remains insoluble upon secretion, but undergoes a rapid change of state (mediated by Ca^{++} and involving uptake of H_2O by the structure) to give an extended extracellular form which is also an ordered array.

The crystalline contents of the secretory vesicle have a precise shape (see Fig. 1 *A*). On average ~3 μm long and 1 μm across at the widest point, the body of a trichocyst (intracellular form) is shaped like a carrot with an elaborate tip at the wide end, by which it is attached to preformed cortical sites to await exocytosis. This shape may be altered by single gene mutation (Pollack, 1974; Ruiz et al., 1976; Cohen and Beisson, 1980) or by action of the carboxylic ionophore monensin (Adoutte et al., 1984), which specifically raises the pH of the Golgi apparatus and Golgi-derived vesicles (Tartakoff, 1983). The extracellular, or extended trichocyst form is that of a needle, on average 25 μm long and 0.7 μm wide (see Fig. 1 *B*). The trichocyst tip does not extend.

Thin sections of fixed and embedded *Paramecia* first revealed the crystalline organization of trichocysts as well as their site of assembly in cytoplasmic vesicles (and not at the cortical exocytotic sites where mature trichocysts ultimately attach; Yusa, 1963; Ehret and De Haller, 1963; Selman and Jurand, 1970). A regular pattern of bands at right angles to the long axis of the trichocyst, with a periodicity of 70–80 Å, was reported and periodicities were sometimes also observed in other directions. Negative staining of the bodies of condensed trichocysts provides little information because of their thickness, however the trichocyst tip gives a complicated pattern showing fine details. Bannister (1972), on the basis of negative stain images of body and tip, considered the repeat of the transverse banding pattern to be 160 Å.

The most detailed published images of the extended form were obtained by negative staining of extruded trichocysts (Hausmann et al., 1972; Bannister, 1972). In these images the extended trichocysts resemble paracrystals of fibrous alpha proteins such as fibrinogen (Tooney and Cohen, 1977) or tropomyosin (Caspar et al., 1969). There are dense bands at right angles to the long axis of the trichocyst every 550–600 Å. However, close examination of the "interband" pattern, which alternates, reveals a true repeat every two bands (1,200 Å) while Bannister (1972) has interpreted the scalloped appearance of the edges of the trichocysts in some images as evidence of a 2,400-Å "super-periodicity". These authors have noted the "eightfold stretching" of trichocysts upon exocytosis and expected to find a factor of 8 in the ratio of the transverse-banding patterns of the two forms.

Most microscopists have commented upon the fact that trichocysts appear to be built up from fibrous elements. Upon heating (Pollack and Steers, 1973; Peterson et al., 1987) or extensive dialysis against distilled H_2O (Steers et al., 1969; Hausmann et al., 1972), trichocysts tend to dissociate and it is possible to observe detached fibrils. Yet, at present, there is no biochemical evidence that trichocysts are composed of fibrous proteins, indeed, an astonishingly complex pattern of

acidic polypeptides of rather low molecular mass characterizes these organelles. SDS-PAGE of purified trichocysts reveals several major bands of M_r 15–20 kD and a few minor bands with M_r from 20 to 25 kD. Isoelectric focusing separates each major band into many bands differing by their charge, in a pI range of roughly 4.5–5.5, so that on a two-dimensional gel as many as 100 polypeptides may be distinguished (Adoutte et al., 1980; Tindall, 1986). Moreover, posttranslational modifications such as glycosylation or phosphorylation have never been detected (Steers et al., 1969; Adoutte, 1987). Possible explanations for this amazing complexity include multiple gene copies, recombination at the level of the micronuclear to macronuclear differentiation, intracellular proteolysis, posttranslational modifications other than glycosylation or phosphorylation, or, perhaps, chemical artifact.

Despite difficulties in stabilizing condensed trichocysts in vitro, preparations of condensed trichocysts, devoid of their membranes, have been obtained in solutions usually containing Mg^{++}, EGTA, and sucrose (Steers et al., 1969; Anderer and Hausmann, 1977; Bilinski et al., 1981; Garofalo and Satir, 1984). It has been reported that in vitro, the transition from the condensed to the expanded form requires Ca^{++} (of the order of 10^{-6} M at pH 7) and is furthermore pH dependent; the more acid the pH, the higher the Ca^{++} concentration required (Garofalo and Satir, 1984). In vivo, expansion of the crystalline contents of the secretory vesicle has also been reported to require Ca^{++} (Matt et al., 1980), which normally enters the vesicle from the external medium upon fusion of the vesicle membrane with the plasma membrane. (For a review of exocytosis in *Paramecium*, see Adoutte, 1987.) Once the membrane fusion has occurred, the explosive trichocyst expansion may serve to propel the contents of the vesicle out of the cell.

We have undertaken a structural study of *Paramecium* trichocysts in order to understand the mechanical features of this unusual organelle in terms of molecular design. Here we present x-ray diffraction patterns and freeze-etching and freeze-fracture images of isolated, untreated trichocysts. On the basis of these data we can propose a crystal lattice for both condensed and extended trichocysts. The unit cells of both forms are of surprisingly large dimensions and have a very high solvent content.

Materials and Methods

Isolation of Trichocysts

Culture Conditions. *Paramecium tetraurelia* wild type stock d4-2 was grown in Wheat Grass Powder (Pines International, Lawrence, KA), bacterized with *Aerobacter* aerogenes, at 27°C to the beginning of stationary phase (2,000–4,000 cells/ml). Cultures were then transferred to 18°C for 1–3 d, where the cells probably divided once more.

Condensed Trichocysts. Depending upon the amount of material required, 2–5 liters of culture were collected by continuous flow centrifugation or by centrifugation in pear-shaped bottles in an oil-testing centrifuge at 300 *g*. The cells were washed in 250 ml ice-cold TEK buffer (20 mM Tris, 5 mM EGTA, 100 mM KCl, pH 7; Garofalo and Satir, 1984) and collected by centrifugation at 300 *g* four times. The final washed cell pellet was taken up in 4–5 ml PHEM-100 mM $MgCl_2$ per ml cell pellet (PHEM[1]: 60 mM Pipes, 25 mM Hepes, 10 mM EGTA, 2 mM $MgCl_2$, pH 6.9; Schliwa and Van Blerkom, 1981), the volume of the suspension was measured and Triton X-100 added from a freshly prepared 20% stock solution to bring the cell suspension to 1% in Triton X-100. The cell lysis buffer and all subsequent buffers contained 1 mM azide. Sometimes 50 μM/ml phenylmethylsulfonyl fluoride and 5 μM/ml leupeptin were also added; their presence or absence did not modify the SDS-PAGE gel profile or the x-ray diffraction patterns of the purified trichocysts (data not shown), so they were not generally included.

The cell suspension was left for 90–120 min on ice and all subsequent steps were carried out on ice, in a cold room. After incubation in the cell lysis buffer the suspension was gently homogenized (10–20 strokes) in a glass–teflon homogenizer to completely disrupt the cell cortex and centrifuged 5 min at 3,500 rpm in a rotor (SS-34; Sorvall Instruments, Newton, CT). The pellet was resuspended in 2–3 ml of PHEM/100 mM $MgCl_2$/0.25 M sucrose with a Pasteur pipette, and layered on 50% Percoll (Pharmacia, Inc., Uppsala, Sweden)/PHEM/100 mM $MgCl_2$/0.25 M sucrose, usually on 10 gradients of 10 ml, which were then centrifuged 15 min in a rotor (50 TI; Beckman Instruments, Inc., Palo Alto, CA) at 27,500 rpm (50,000 *g*). Sometimes gradient marker beads (Pharmacia, Inc.) were included in a separate tube to calibrate the gradient. Condensed trichocysts form a sharp band 1.5–2 cm from the bottom of the tube while bits of cortex band 4–5 cm from the bottom of the tube and extended trichocysts.

The condensed trichocyst bands were carefully removed with a Pasteur pipette. The volume was measured and diluted with 5 vol of PHEM/100 mM $MgCl_2$/0.25 M sucrose and centrifuged in a rotor (SS-34; Sorvall Instruments) at 13,000 rpm for 20 min. The Percoll forms a hard pellet and the trichocysts a very loose pellet. The trichocysts were then washed three times in 20 ml of PHEM/100 mM $MgCl_2$/0.5 M sucrose. Such preparations contain very nearly 100% condensed trichocysts, which of course lack membrane and also lack the outer sheath. Some preparations were contaminated by a few micronuclei or fragments of macronuclei.

For x-ray diffraction experiments the washed trichocysts were centrifuged at 5,000 rpm in an Eppendorf tube in a microfuge (MLW, Liepzig, German Democratic Republic), then transferred with a drawn out glass capillary to a 1 mm quartz capillary. x-ray experiments were carried out at 10°C.

Extended Trichocysts. Extended trichocysts were prepared by the method described above, except that the buffers contained 20 mM $MgCl_2$ rather than 100 mM $MgCl_2$. It was necessary to lower the Mg^{++} concentration, otherwise some trichocysts do not extend upon dilution into a low ionic strength buffer containing $CaCl_2$. Extended trichocyst preparations were contaminated by a very small proportion of isolated kinetodesmal fibers.

Instead of washing the loose trichocyst pellet (first step after Percoll gradient) in a high Mg^{++}, high sucrose buffer, the trichocysts were diluted into 20 ml 1 mM $CaCl_2$, which triggers the transition to the extended form, and the extended trichocysts were then washed at least two more times with 20 ml 1 mM $CaCl_2$.

From time to time, preparations of trichocysts were examined on SDS-polyacrylamide gels according to the protocol of Thomas and Kornberg (1975). Both the condensed and the extended trichocysts gave the same gel profile on these one-dimensional SDS gels. Others have found no difference in the protein composition of the two forms using high resolution two dimensional gels (Peterson et al., 1987).

Glutaraldehyde Fixation of Trichocysts. To a suspension of either condensed or extended trichocysts in 20 ml of the appropriate final wash buffer, 70% glutaraldehyde (Ladd Research Industries, Inc., Burlington, VT) was added to bring the glutaraldehyde concentration to 0.1% and the suspension was left for at least 3 d in the cold room. The trichocysts were then centrifuged and washed at least three times in 10 mM Tris-HCl, pH 8. The trichocyst pellets were light yellow in color.

Determination of the Density of Trichocysts

Density marker beads (Pharmacia, Inc.) were used as suggested by the manufacturer to calibrate the self-forming Percoll gradients. The density of glutaraldehyde-fixed yeast flavocytochrome b_2 crystals was measured in the same way as the density of trichocysts. In gradients containing 0.15 M NaCl, the flavocytochrome b_2 crystals had a density of 1.133 g/ml, consistent with density measurements performed in polyethylene glycol 8000 (1.13–1.14 g/ml) and with the crystal structure (Xia et al., 1987), but not with earlier measurements made on glutaraldehyde fixed crystals using mixtures of organic solvents (Mathews and Lederer, 1976).

X-ray Diffraction

Most of the experiments were performed with an Eliott rotating anode generator, a camera with line collimation geometry and a linear position sensitive detector with a conductive wire (Sardet et al., 1976). Experiments

1. *Abbreviations used in this paper*: PHEM, 60 mM Pipes, 25 mM Hepes, 10 mM EGTA, 2 mM $MgCl_2$, pH 6.9; W-Ta, Tungsten-Tantalum.

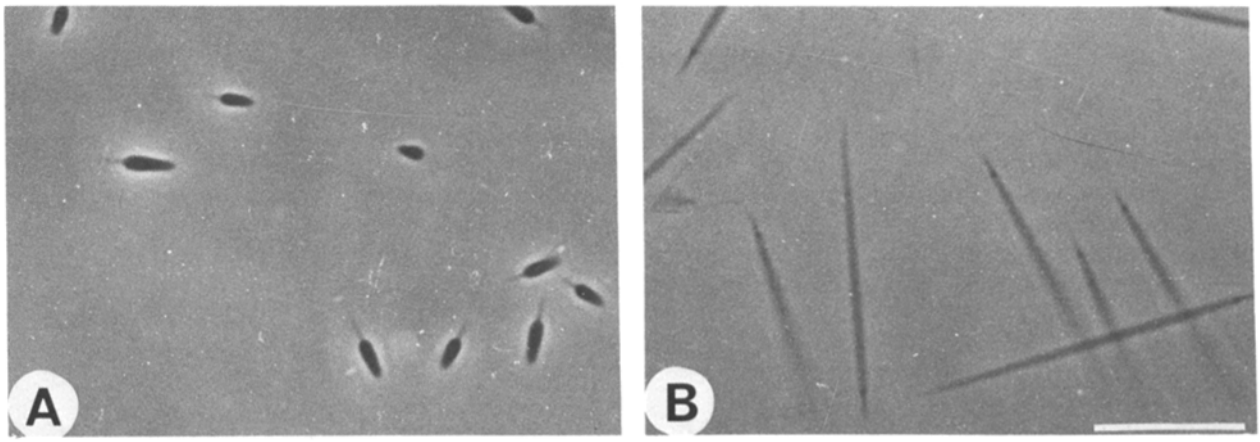

Figure 1. Phase contrast light microscope images of isolated, untreated trichocysts. (*A*) Condensed trichocysts and (*B*) extended trichocysts. Note that the bodies of condensed (but not of extended) trichocysts are highly birefringent. Bar, 10 μm.

were also performed using synchrotron radiation at LURE (Laboratoire pour l'Utilisation du Rayonnement Electromagnétique, Orsay, France) on the D24 small angle camera which has point collimation. A linear position sensitive detector with delay line readout was used to collect the data at LURE. The prototype D11 camera has been described by Koch et al. (1982).

Freeze-etching and Freeze-Fracture Electron Microscopy

The results presented here were obtained using untreated, concentrated preparations of condensed and extended trichocysts. To assure good freezing of such samples, two ultrarapid freezing procedures were used.

The first one is a modification of the previously described "sandwich" technique (Aggerbeck and Gulik-Krzywicki, 1986). A very thin layer of the sample is spread on a flat copper plate and immediately covered with a similar, but intentionally irregular, upper plate to form regions of close contact separated by "pockets" of solution not adhering to the upper plate. This sandwich is then rapidly plunged into liquid propane. The opening of these two plates at −150°C, under a vacuum of about 10^{-7} Torr in a freeze-fracture unit (BAF 301) produces fractures in the frozen solution. In some places, corresponding to the above-mentioned pockets, the solution is not fractured, and a thin layer of fully hydrated trichocysts is exposed instead.

In the second procedure, designed for ultrarapid mixing followed by ultrarapid freezing of suspensions of particles (Gulik-Krzywicki, T., and Y. Dupont, to be described in detail elsewhere), a suspension of trichocysts was forced through a small hole to give a very fine stream, which was projected onto a metal surface that nebulized it to produce a cloud of very small droplets (10–50 μm diam) that was immediately frozen in liquid propane. The fracturing of these droplets was performed by the procedure currently used for spray freezing (Bachmann and Schmitt-Fumian, 1973).

We found that the modified sandwich method could not provide fractures perpendicular to the trichocyst long axis, probably because of the preferred longitudinal orientation of the organelles when flattened between two copper plates. The modified "spray" method was therefore used to obtain cross-fractures.

Replication of the fractured, fractured and etched, or simply etched trichocysts was performed using Tungsten-Tantalum (W-Ta) alloys in four to six steps, each lasting a few seconds and separated by ~10-s periods during which the partly shadowed surfaces were allowed to cool. Some samples were shadowed unidirectionally and others were rotary shadowed in a conventional way (Aggerbeck and Gulik-Krzywicki, 1986). To avoid contamination of the surfaces, the samples were protected between each shadowing step by a liquid nitrogen–cooled knife. The replicas were cleaned in chromic acid, washed with distilled water, and observed in a Philips 301 electron microscope.

Results

Isolation of Trichocytes

A physical study of *Paramecium* trichocysts begins with the isolation of the organelle. For x-ray diffraction in particular, stable homogeneous populations of each form in relatively large amounts (at least a few milligrams) are required. In return, the x-ray experiments provide a rapid and sensitive way of monitoring the quality of the preparation, and this was indispensible to us in the development of an isolation procedure.

The previously published procedures for the isolation of condensed trichocysts[2] (Bilinski et al., 1981; Garofalo and Satir, 1984) gave in our hands mixtures of the condensed form, "false discharge" forms (the condensed trichocysts swell in all directions to give amorphous structures of low birefringence; see Bannister, 1972) and a few discharged trichocysts, more or less contaminated by other cellular structures. Extended trichocysts may be collected after exocytosis (Rauh and Nelson, 1981) but such an approach was found unsatisfactory because of the low yield.

Our strategy originated from the observation that trichocysts remain condensed under the conditions routinely used in our laboratory for immunocytochemical studies: PHEM buffer (see Materials and Methods) of Schliwa and Van Blerkom (1981), 1% in Triton X-100. In this buffer-detergent system, especially in the presence of additional $MgCl_2$, the usually robust cell cortex dissociates to leave trichocysts, minus their membrane and outer sheath, as essentially the only intact structure in the lysed cell suspension. They can then be easily and rapidly separated from all the other cell debris on self-forming Percoll gradients. Extended trichocysts were prepared by dilution of condensed trichocysts into a low ionic strength buffer containing Ca^{++}. The preparative procedure is described in detail in Materials and Methods. The appearance in the phase contrast microscope of condensed and extended trichocysts isolated in this way is shown in Fig. 1.

Although they have been prepared under conditions that certainly release intracellular proteases, the trichocyst "crystalline matrix" we purify appears structurally intact as judged by x-ray diffraction and electron microscopy, while the proteins, visualized by Coomassie Blue staining of heavily overloaded SDS gels (data not shown), do not appear to be degraded and give the usual profile (Adoutte et al., 1984). The ability of the trichocysts to extend in vitro provides an addi-

2. For simplicity's sake, what should more correctly be referred to as the trichocyst contents we shall denote by "trichocyst."

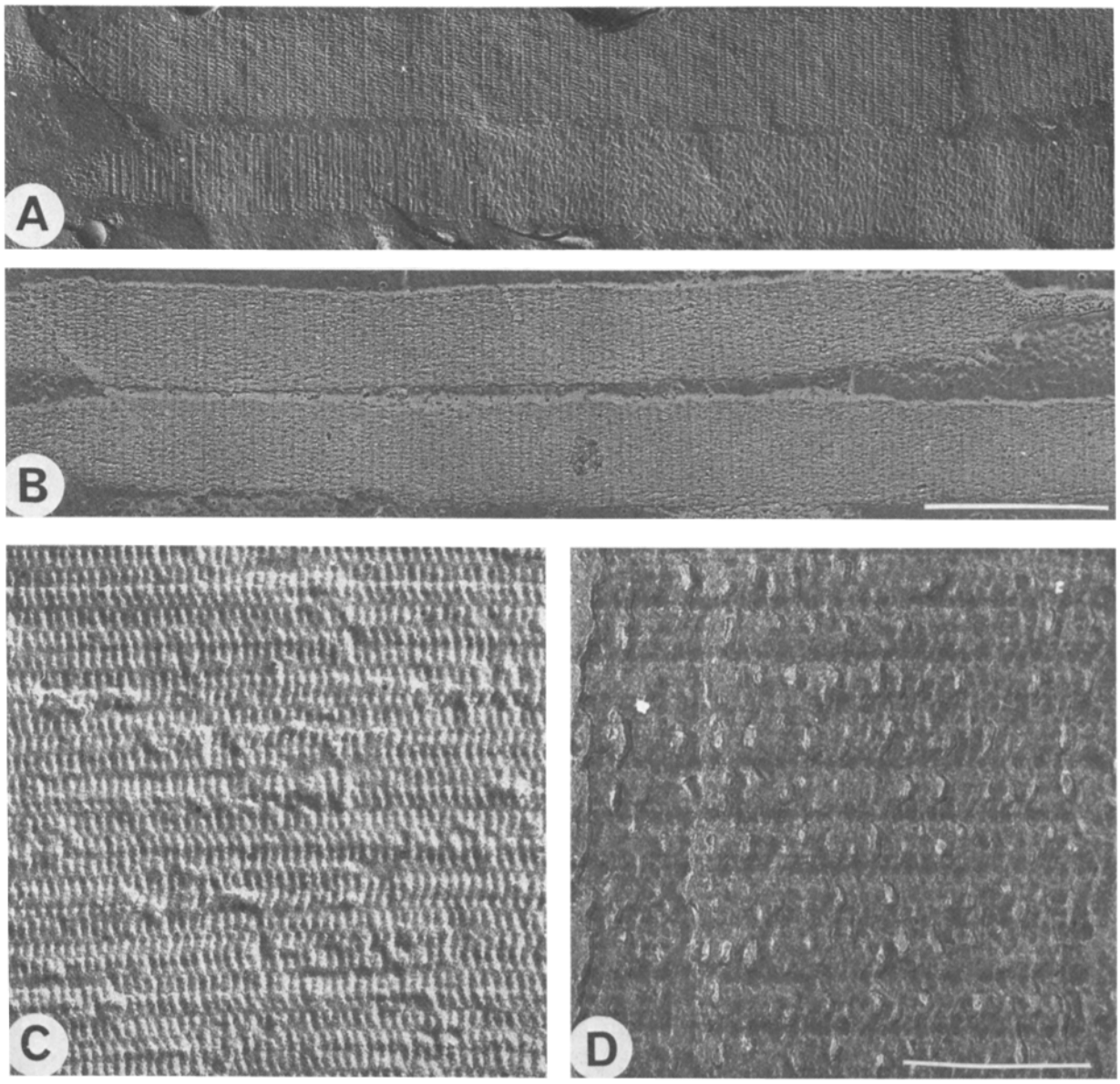

Figure 2. Freeze-fracture electron micrographs of well-frozen and poorly frozen extended trichocysts. Both samples were fractured at −125°C, etched for 3 min at −105°C under a vacuum of $\sim 10^{-7}$ torr, and unidirectionally (*A* and *C*) or rotary (*B* and *D*)-shadowed with Tungsten-Tantalum (W-Ta). (*A* and *C*) Typical low and high magnification views of well frozen samples. (*B* and *D*) Similar views of poorly frozen samples. Note the presence of complex, regular patterns in *A* and *C* but only regularly spaced, almost featureless bands in *B* and *D*. Bars: (*B*) 1,000 nm; (*D*) 200 nm.

tional argument for the integrity of their constituent polypeptides.

Freeze-Etch and Freeze-Fracture Electron Microscopy

One reason for choosing freeze-etch and freeze-fracture techniques is that the native trichocysts are too thick for either negative staining or cryomicroscopy of frozen hydrated specimens, the techniques usually used for structural studies of ordered assemblies of macromolecules. An advantage of freeze-etch and freeze-fracture methods is that the images obtained reflect local structure (surface of the organelle or the structure at a given fracture plane) and not the projection (superposition) of the whole structure of the organelle.

A particular effort has been devoted to obtaining high quality images of the same untreated preparations studied by x-ray diffraction. Conventional freeze-drying and freeze-fracture were found to be inadequate for such preparations, since they produced important alterations of the trichocyst morphology.

Both of our ultrarapid freezing methods, modified sandwich and modified spray, gave reproducible high-quality images with condensed trichocyst preparations. Good preservation of the extended trichocysts could be assured by the use of cryoprotectants (such as glycerol or sucrose) but such treatment precludes etching, which is important for understanding the morphology of the object under study. The quality and the reproducibility of the results obtained with extended trichocysts in the absence of a cryoprotectant were much less satisfactory than the results obtained with condensed trichocysts under comparable conditions. The difficulty in preserving native structure probably results from the very high solvent content of extended trichocysts (>90%; see

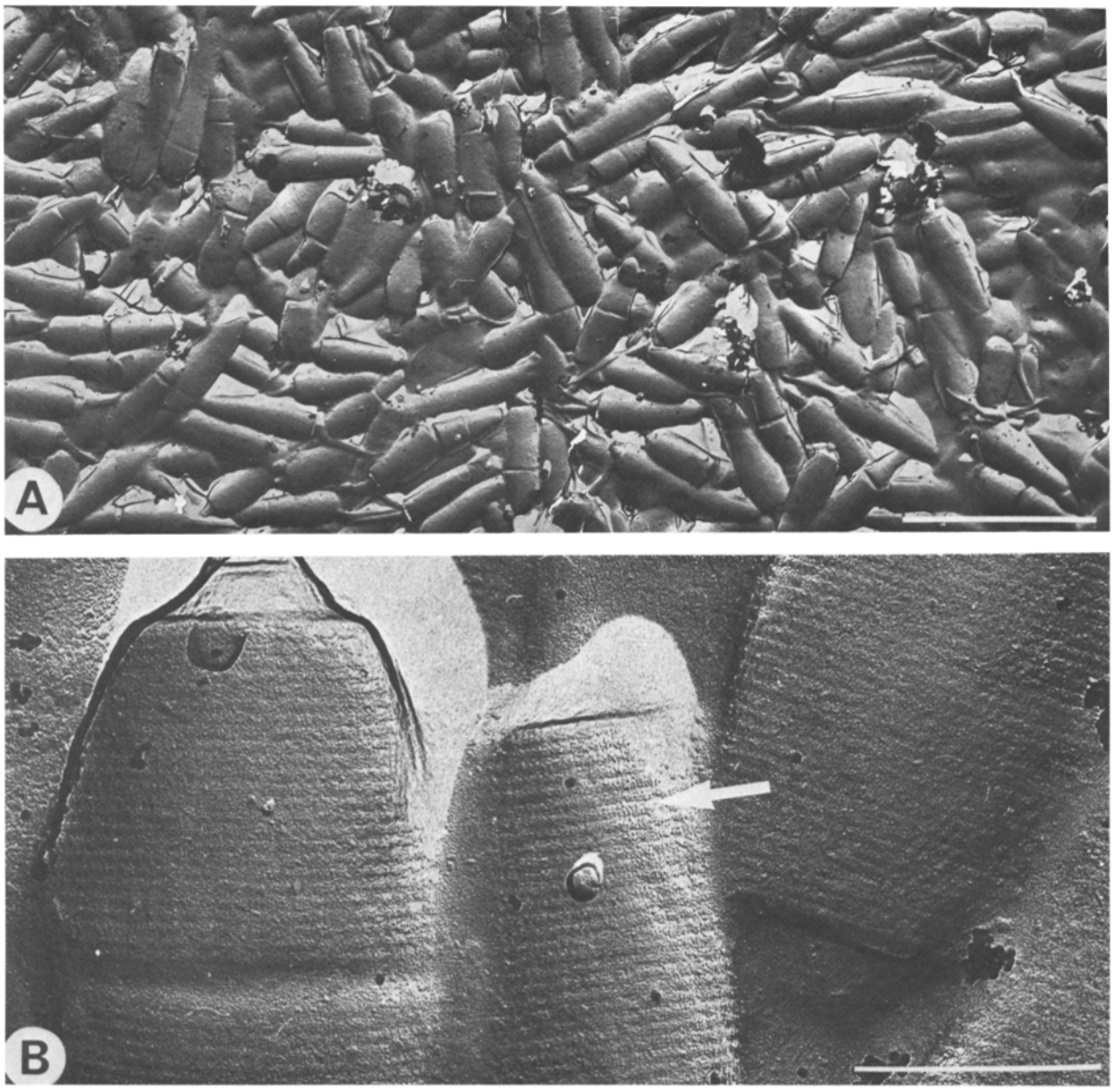

Figure 3. Freeze-etch images of unfractured, condensed trichocysts. The sample was etched for 6 min at −105°C under a vacuum of ~10^{-7} torr, then unidirectionally shadowed with W-Ta. The homogeneity of the preparation can be deduced from the low magnification view in *A*. Note the regularly spaced bands perpendicular to the trichocyst long axis and the fine, regular striations parallel to the long axis (*arrow* in *B*). Bars: (*A*) 5,000 nm; (*B*) 500 nm.

below). Most of the untreated, extended trichocyst preparations showed only poor preservation of the original structure, particularly after etching of the fractured surfaces. Examples of such images are shown in Fig. 2, *B* and *D*. Even when special care was taken, few preparations gave truly high quality images such as those shown in Fig. 2, *A* and *C* (see also Figs. 5 and 6 below). The reason for this irreproducibility is currently under study; we are probably close to the limits of the technique given the intrinsic fragility of the organelle which may arise, in part, from its very high water content.

Determination of the Crystal Lattice

We sought to determine the crystal forms of condensed and extended trichocysts by combining the information obtained from x-ray diffraction powder patterns and from freeze-fracture and freeze-etch electron microscope images.

Surface views of condensed trichocysts, as revealed by freeze-etching of unfractured parts of the sample (see Materials and Methods), are shown in Fig. 3. The low magnification view (Fig. 3 *A*) indicates the high degree of homogeneity of the preparation. Higher magnification views clearly show regularly spaced bands perpendicular to the long axis of the trichocyst at 300-Å intervals, and in some regions (see *arrow* in Fig. 3 *B*) regular striations parallel to the long axis.

Freeze-fracture of condensed trichocysts reveals three privileged fracture planes corresponding to three distinct two-dimensional patterns; examples are shown in Fig. 4. The view most often found (Fig. 4 *A*) is characterized by a period of ~320 Å in the direction of the trichocyst long axis. In the

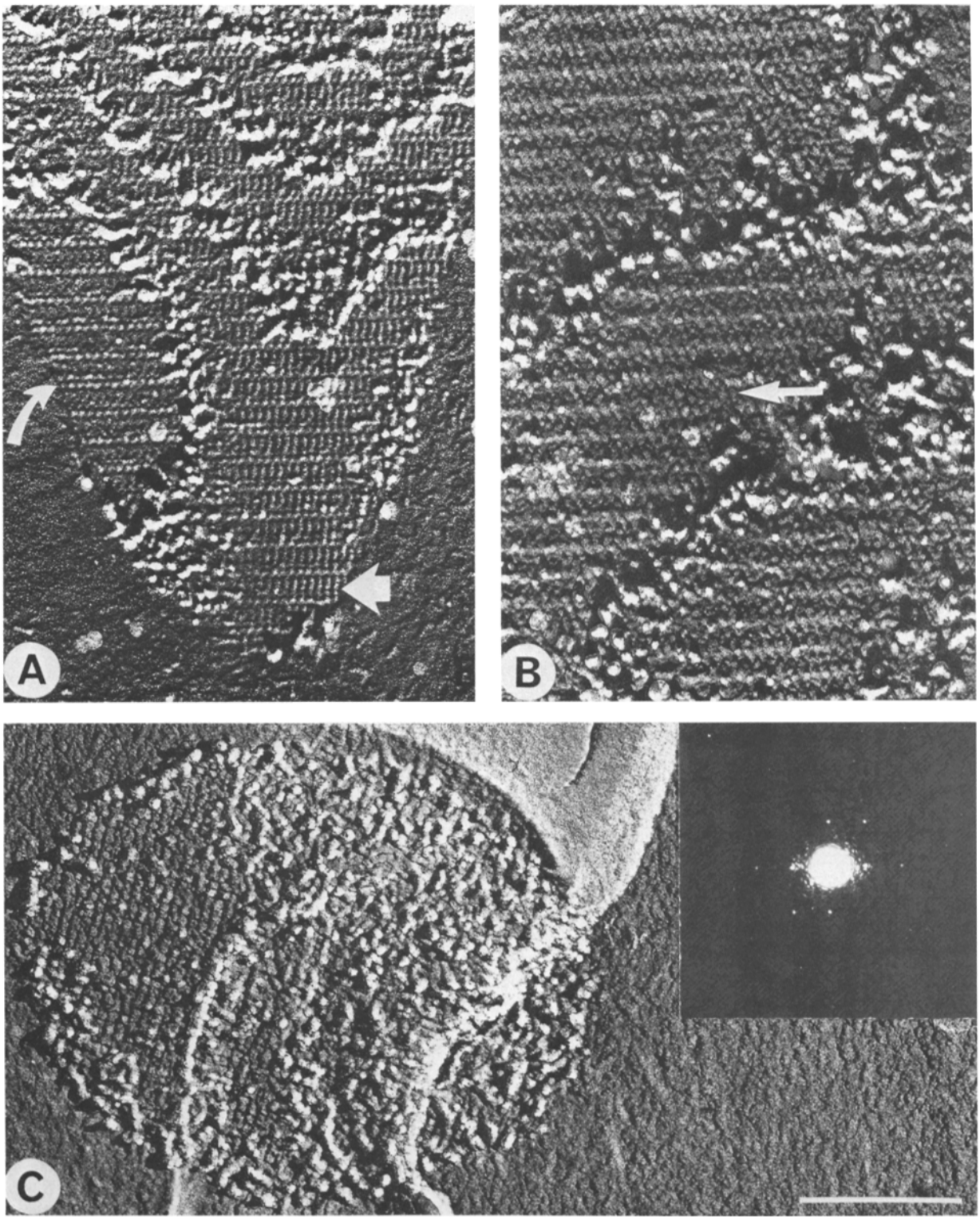

Figure 4. Freeze-fracture images of condensed trichocysts. The samples were fractured at −125°C under a vacuum of $\sim 10^{-7}$ torr and unidirectionally shadowed with W-Ta. The contrast in these micrographs is inverted (shadow is black). (*A* and *B*) Views of longitudinal fractures and (*C*) of a cross-fractured trichocyst. Note the presence of complex, regular two-dimensional net arrays of what look like short filaments, some of which are parallel (*large arrow* in *A*), others perpendicular (*curved arrow* in *A*), and still others tilted (*arrow* in *B*) with respect to the trichocyst long axis. (*Inset*) Optical diffraction of the ordered portion of the same cross-fractured trichocyst allowing measurement of the rectangular lattice: 106 Å × 127 Å. Bar, 200 nm.

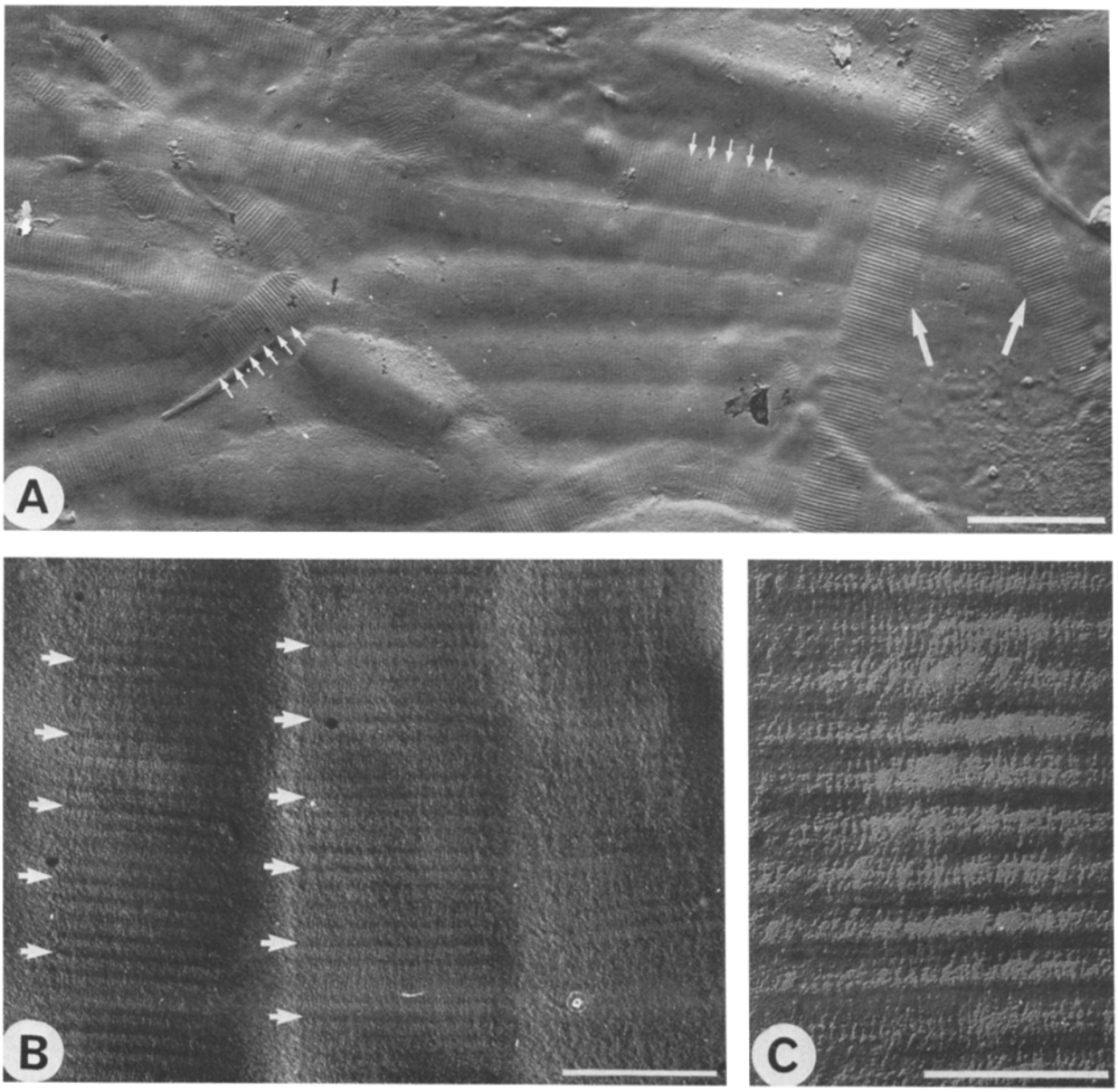

Figure 5. Freeze-etch view of unfractured, extended trichocyst preparations. The sample was etched for 6 min at −105°C under a vacuum of ~10^{-7} torr and unidirectionally shadowed with W-Ta. Note morphological differences between lightly etched (*small arrows* in *A* and *B*) and collapsed (*large arrows* in *A*) trichocysts. Lightly etched trichocysts show much more complex surface structure than collapsed ones. The former show repeating morphological units every four bands (*small arrows* in *A* and *B*) and quite regular striations parallel to the trichocyst long axis (*C*) while the latter show only regularly spaced bands separated by deep grooves. Bars: (*A*) 2,000 nm; (*B*) 500 nm; (*C*) 200 nm.

other direction filaments are seen, packed side to side every ~105 Å. Measurement of the periodicities of a large number of examples of the pattern shown in Fig. 4 *A* gave values of 300–330 Å the length of the trichocyst and 99–113 Å for the side to side packing, with an angle between the two axes close to 90°.

Fig. 4 *B* is the second pattern found. The two-dimensional lattice has dimensions of 314–330 and 126–140 Å, with an angle between the axes of ~90°. Filaments appear to traverse this rectangular lattice at an angle of 65–70°.

Finally, Fig. 4 *C* shows a fracture perpendicular to the trichocyst long axis. In the ordered regions, one finds an approximately rectangular lattice of dimensions 100–111 Å × 125–135 Å (see optical diffraction [*inset*]).

If these fractures correspond to the principal planes of the crystal, then we have an orthorhombic or monoclinic unit cell with one dimension of ~320 Å and the other two dimensions between 100 and 140 Å. It is also possible that the fractures in Fig. 4, *A* and/or *B* run along diagonals of the unit cell.

Freeze-etch views of unfractured, extended trichocysts are shown in Fig. 5. The low magnification view (Fig. 5 *A*) shows highly elongated objects displaying very regularly spaced bands at 550-Å intervals. These bands are separated by

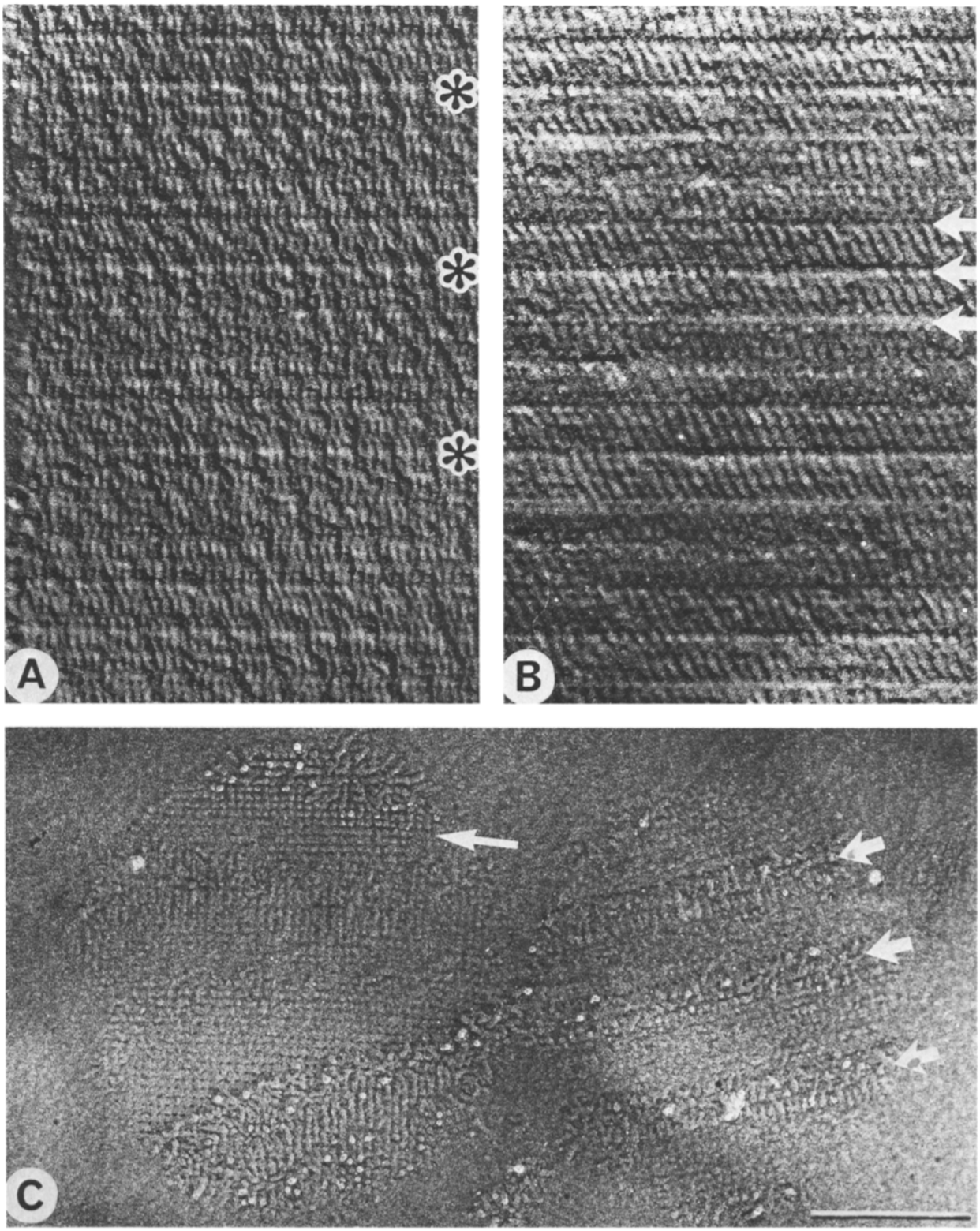

Figure 6. Freeze-fracture electron micrographs of extended trichocysts. The samples were fractured at −125°C, etched for 3 min at −105°C, and unidirectionally (*A* and *B*) and rotary (*C*)-shadowed with W-Ta. The contrast in these micrographs is inverted (shadow is black). (*A* and *B*) Typical longitudinal fractures and (*C*) cross-fractures. Note the presence of filament-like elements, some of which are parallel (*A*) and others tilted (*B*) with respect to the trichocyst long axis. Note also the repeating morphological units every four striations (*asterisks*). Arrow in *C* points to a regular square lattice which appears between two more or less wide stripes; such stripes correspond to the regularly spaced 570-A striations seen on the longitudinal fractures, as indicated by the thick arrows on a trichocyst fractured at a slightly oblique angle. Bar, 200 nm.

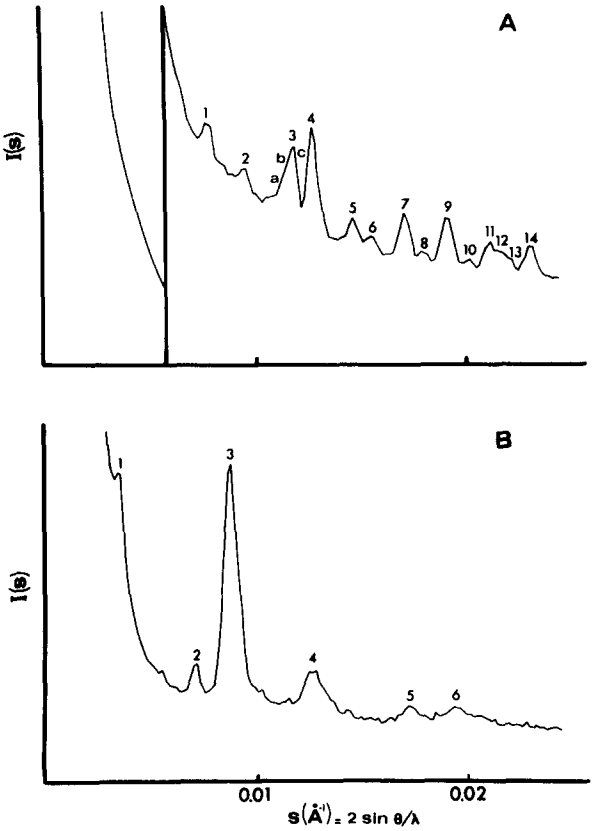

Figure 7. X-ray diffraction patterns of isolated, untreated, unoriented trichocysts. (*A*) Condensed trichocysts; (*B*) extended trichocysts. These spectra were recorded on the D24 small-angle camera at LURE (Orsay, France) using synchrotron radiation. The x-ray wavelength in this experiment was 1.608 Å and the specimen to detector distance 1 m. The intensity scale is in arbitrary units. 2θ is the scattering angle.

grooves that become deeper and deeper as a function of the collapse of the trichocysts due to freeze-drying (see the *large arrows* in Fig. 5 *A*, pointing at two particularly dry trichocysts). Higher magnification views (Fig. 5 *B*) of the lightly freeze-etched trichocysts show a more complex pattern that repeats every four bands or 2,200 Å (see *small arrows* in Fig. 5, *A* and *B*). The enlargement shown in Fig. 5 *C* reveals striations parallel to the trichocyst long axis, spaced ~100 Å apart.

Fig. 6 shows some longitudinal and cross-fractures of extended trichocysts. There is a periodicity of roughly 570 ± 10 Å along the length of the trichocysts (Fig. 6, *A* and *B*) and a square lattice of ~115 ± 5 Å elements in the plane perpendicular to the long axis (Fig. 6 *C*). On oblique fractures, the square lattice is regularly disrupted by a variable number of more or less wide "stripes" as can be seen on the two almost perpendicularly cross-fractured trichocysts in Fig. 6 *C*. If we assume that the stripes are the 570-Å transverse striations, then their thickness and number in the oblique sections, which are a function of the angle of fracture, are what one would expect if the crystal lattice of extended trichocysts were orthorhombic, with dimensions of ~570 × 115 × 115 Å. On most of the longitudinal sections a super periodicity corresponding to 4 × 570 Å (~2,300 Å) is clearly visible (see Fig. 6, *A* and *B* as well as Fig. 2 *B* for the low magnification view). The same super periodicity is also observed on the longitudinal fractures of cryoprotected extended trichocysts (not shown). It thus seems very probable that the true unit cell of extended trichocysts has dimensions close to 2,300 × 115 × 115 Å.

We now turn to the x-ray patterns of unoriented samples of condensed and extended trichocysts, shown in Fig. 7. Data were collected over the angular range (1/600) $Å^{-1} < s <$ (1/40) $Å^{-1}$ ($s = 2\sin\theta/\lambda$) but are shown here starting at (1/330) $Å^{-1}$ since no diffraction peaks were observed at smaller s values. Strong scattering near the beam stop results from small amounts of residual Percoll in the trichocyst preparations. The samples diffracted out to $\sim s =$ (1/20) $Å^{-1}$, but only the part of the pattern shown was used for indexing. The peaks in Fig. 7 have been numbered, from 1 to 14 for the condensed trichocyst pattern and from 1 to 6 for the extended trichocyst pattern.

The diffraction peaks are wider than the direct beam and some of the peaks are wider than others. For example (Fig. 7 *A*) if peak 4 is a single major reflection, then peak 3 must represent the superposition of a few major reflections (hence peak 3 has been subdivided into 3 peaks in Fig. 7 *A*). Because of superposition, determination of the positions of the peaks is difficult for the condensed trichocyst pattern. The strikingly simpler extended trichocyst diffraction pattern (Fig. 7 *B*) poses fewer problems.

In our efforts to index the condensed trichocyst pattern, we looked for a scheme consistent with the electron microscope results which could account for all of the diffraction peaks. We found several possible monoclinic unit cells. They had in common one dimension ~320 Å, a second dimension between 130 and 145 Å, and a third dimension between 95 and 112 Å. We also tried to index the pattern using an automatic indexing program (Taupin, 1968). To our surprise, despite the uncertainties (large estimated errors) in the peak positions, the program found only a few (~10 different) ways to account for all the reflections. Only one of them (a = 111 Å, b = 130 Å, c = 330 Å, γ = 86°) seemed to be compatible with the electron microscopy, and it also happened to have a significantly better figure of merit than the other schemes found by the indexing routine; it is shown in Table I. In this indexing scheme, the strongest reflections (peaks 3 *c* and 4) are the 111 and 1-11 diagonals. The fractures shown in Fig. 4 thus correspond to the principle planes of the crystal: the $a \times c$ plane (Fig. 4 *A*), the $b \times c$ plane (Fig. 4 *B*), and the $a \times b$ plane (Fig. 4 *C*).

The relatively simple extended trichocyst pattern (Fig. 7 *B*) is indexed with no difficulty as shown in Table II. The x-ray reflections correspond to diffraction from 001 and hk0 planes of a lattice with $a = b$ = 115 Å and c = 571 Å. Since no reflections could be unambiguously identified as hkl reflections, it is not possible to determine the angle between the square lattice and the longitudinal repeat. Furthermore, as the first order of a 2,300-Å dimension would not have been observed under our experimental conditions (such small s values are very difficult to record in x-ray diffraction experiments) and since a dimension of 571 Å allows us to index all observed reflections, it is not possible to tell whether the true repeat is 571 Å or a multiple thereof. The freeze-fracture images agree with these unit cell dimensions and provide complementary information: the true longitudinal repeat is most likely to be 4 × 571 Å = 2,300 Å and the angle between the square lattice and this dimension is close or identical to

Table I. Condensed Trichocyst Indexing Scheme

Peak	s observed	s calculated	h	k	l
1	0.0077	0.00770	0	1	0
2	0.00950	0.00952	1	0	1
3a	0.01090	0.01087	1	0	2
3b	0.01140	0.01143	1	1	0
3c	0.01175	0.01183	1	1	1
4	0.01265	0.01264	1	−1	1
5	0.01460	0.01461	1	1	3
6	0.01540	0.01527	1	−1	3
6	0.01540	0.01540	0	2	0
7*		0.01655	0	2	2
7	0.01700	0.01701	0	1	5
7*		0.01728	1	2	0
8	0.01790	0.01788	0	2	3
8	0.01790	0.01804	2	0	0
9	0.01910	0.01899	1	1	5
9	0.01910	0.01903	2	0	2
9	0.01910	0.01910	2	1	0
10	0.02020	0.02004	2	1	2
10	0.02020	0.02011	2	−1	0
10	0.02020	0.02020	2	0	3
10	0.02020	0.02031	1	0	6
10	0.02020	0.02034	2	−1	1
11	0.02110	0.02101	2	−1	2
11	0.02110	0.02111	1	2	4
11	0.02110	0.02116	2	1	3
11	0.02110	0.02123	0	0	7
12	0.02150	0.02149	1	1	6
12	0.02150	0.02161	0	2	5
13	0.02200	0.02195	1	−1	6
13	0.02200	0.02203	1	−2	4
13	0.02200	0.02207	2	−1	3
14	0.02300	0.02287	2	2	0
14	0.02300	0.02299	1	2	5
14	0.02300	0.02307	1	0	7
14	0.02300	0.02307	2	2	1
14	0.02300	0.02309	0	3	0

hkl are the indices of a reciprocal lattice calculated on the basis of a monoclinic unit cell with A = 111.1 Å, B = 130.2 Å, C = 329.7 Å, and γ = 85.9°. Missing reflections are not included in the table. s is in Å^{-1}.
* Peak 7 appears to be multiple and the 0 2 2 and 1 2 0 reflections may contribute to it.

Table II. Extended Trichocyst Index Scheme

Peak	s observed	s calculated	h	k	l
1	0.0035	0.0035	0	0	2
2	0.0070	0.0070	0	0	4
3	0.0087	0.0087	1	0	0
			0	1	0
4	0.0125	0.0123	1	1	0
		0.01234	1	0	5
		0.01243	1	1	1
5	0.0173	0.0174	2	0	0
			0	2	0
6	0.0195	0.01945	2	1	0
			1	2	0

This index scheme is calculated on the basis of an orthorhombic unit cell with $A = B$ = 115 Å, C = 571 Å. Missing reflections are not included in the table. s is in Å^{-1}.

90°. The trichocysts in Fig. 6 *C* have been fractured at or very near the plane of the 115-Å square lattice while the fractures in Figs. 2 *C* and 6 *A* probably correspond to views of the $a \times c$ plane. Since the side to side packing is 115 Å for the trichocyst in Fig. 6 *A* but 165 Å for the trichocyst in Fig. 6 *B*, the latter is likely to have been fractured along a unit cell diagonal (165 Å would be the diagonal of a 115 Å square).

Unit cell parameters are summarized in Table III. The elementary unit cells which we have determined for the two forms are represented schematically in Fig. 8.

The Contents of a Unit Cell

How much protein is in the unit cell? The densities of condensed and extended trichocysts were measured on Percoll gradients and the results are summarized in Table IV. That Percoll density gradients can be a reliable method for measuring the density of protein crystals was verified by measuring the density of crystals of yeast flavocytochrome b_2, of known structure and density (see Materials and Methods).

Measurements on freshly prepared trichocysts were made in the presence of sucrose. Densities of trichocysts fixed in 0.1% glutaraldehyde were measured on gradients containing 0.15 M NaCl (the standard condition for the density marker beads used for calibration). The higher densities measured in sucrose result from solvent exchange. We can calculate from these density values that condensed trichocysts contain ~70% solvent (30% protein) while extended trichocysts contain at least 90% solvent (<10% protein). The volume fraction of solvent in trichocysts, especially in extended trichocysts, is higher than that found for crystals of globular proteins (Matthews, 1968). However these values would not be unusual for crystals of fibrous proteins (Cohen et al., 1971; Cohen and Tooney, 1974).

The volume fraction of protein decreases by a factor of ~3 in the transition from the condensed to the extended form. This is coherent with the global morphological change in the organelle (Fig. 1), which may be associated with a volume increase of roughly 3, since the extended form is eight times longer but little more than half as wide as the condensed form.

Unit cell volumes calculated from the unit cell parameters are also given in Table IV. The mass of protein in the unit cells of condensed and extended trichocysts may be calculated from the crystal densities and these volumes. The unit cell of a condensed trichocyst contains twice the mass of protein as the unit cell of an extended trichocyst (roughly corre-

Table III. Trichocyst Unit Cell Parameters

Form	*a*	*b*	*c*	γ
	Å			
Condensed	111	130	330	86°
Extended	115	115	571*	90°

Elementary unit cell parameters a, b, and c. γ is the angle between the a and b axes.
* 2,300 Å if we take into account the electron microscope results.

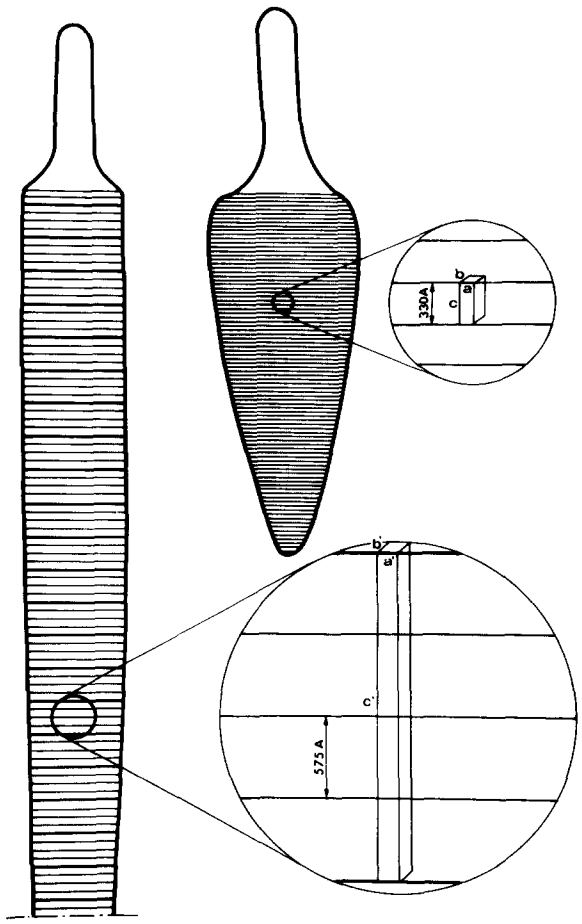

Figure 8. "Cartoon" view of trichocysts. The elementary unit cells proposed for the condensed and extended trichocyst matrix are shown with respect to the intracellular and extracellular forms of the organelle. The drawings are approximately to scale.

sponding to 56 and 28 "monomers" of molecular mass 17,000 daltons), if we take the long dimension to be 571 Å. Of course, if the true longitudinal period of extended trichocysts is 4 × 571 Å, then the unit cell of the extended trichocyst contains twice the mass of protein as the unit cell of the condensed trichocyst.

Trichocyst Tips

So far we have not spoken of the tips of the trichocysts. As they represent only a negligible amount of diffracting material compared with trichocyst bodies, they could be ignored in the interpretation of the x-ray diffraction data. However we can now ask whether the tips have the same structure as the body, a question of some interest since (*a*) tips do not extend under the in vivo or in vitro conditions for body extension and (*b*) single gene mutation can lead to trichocysts whose tips are positioned not at the end but on the side of the body, where they have been likened to the keel of a boat (Pollack, 1974).

Fig. 9 shows some freeze-fracture images of the tip. Fig. 9 *A* is a fracture parallel to the trichocyst long axis; the tip inner sheath is seen in section as a double envelope. The crystalline matrix of body and tip is perfectly continuous and the structure is the same in both regions. Fig. 9 *B* is of the surface of the tip and shows the helical net structure of the inner sheath, which has been described by Bannister (1972). Through the hole in the inner sheath, we recognize a view similar to that identified as the $a \times c$ plane of the condensed trichocyst crystal lattice (Fig. 4 *A*). The body of the trichocyst in Fig. 9 *B* (not shown) is in the extended form. Thus the tip matrix does not extend, perhaps because of the protection from the external medium offered by the inner sheath. This seems all the more likely as Fig. 9 *C* shows that the inner sheath is a very sturdy structure; it has resisted freezing and deep-etching conditions which have destroyed the delicate organization of the extended trichocyst body. We conclude that the tip has the same structure as the rest of the condensed trichocyst, differing in that it is surrounded and protected by the inner sheath.

Discussion

The design and function of *Paramecium* trichocysts pose a number of puzzling questions. How is it possible to build up

Table IV. Density Measurements

Sample	Crystal density	$X_{solvent}$	$V_{unit\ cell}$	$M_{unit\ cell}$*
	g/cm³ ± SD		*Å³ × 10⁻⁶*	*daltons × 10⁻⁵*
Condensed				
PHEM 0.25 M sucrose‡	1.1135 ± 0.002 (4)§	0.71		
Fixed 0.15 M NaCl‖	1.085 ± 0.002 (3)	0.72	4.76	9.4
Extended				
PHEM 0.25 M sucrose‡	1.052 ± 0.003 (3)	0.95		
Fixed 0.15 M NaCl‖	1.027 ± 0.001 (3)	0.92	7.55	4.7

Densities of untreated and of glutaraldehyde fixed trichocysts were measured on self-forming Percoll density gradients. Calibration curves were established with density marker beads purchased from Pharmacia. $X_{solvent}$ is the volume fraction of solvent in the unit cell of volume $V_{unit\ cell}$.
* $M_{unit\ cell}$ is the molecular mass of the unit cell. For molecular mass calculation, it was assumed that the density of the solvent is the same as that of water. This simplification may introduce an error of the order of 5% (Matthews, 1985).
‡ PHEM/100 mM $MgCl_2$/0.25 M sucrose buffer. Densities are higher in sucrose because of solvent penetration. Solvent density is taken to be 1.04 g/liter.
§ Numbers in parentheses are the number of measurements made.
‖ Glutaraldehyde-fixed trichocysts (see Materials and Methods); 0.15 M NaCl buffer. Solvent density is taken to be 1.006 g/liter.

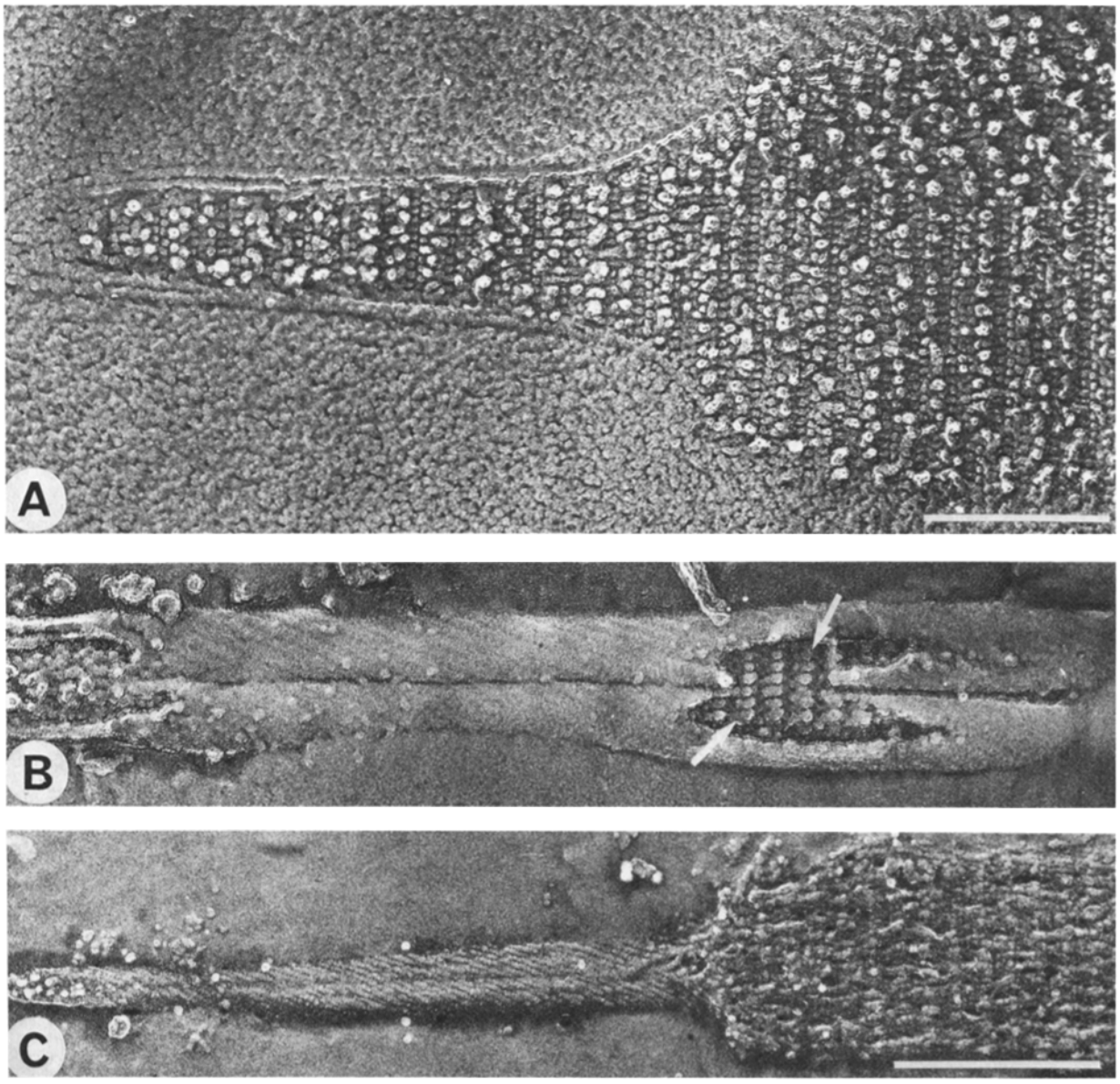

Figure 9. Freeze-fracture electron micrographs of condensed and extended trichocyst tips. The contrast has been inverted (shadow is black). (*A*) Condensed trichocyst, etched for 2 min at −105°C, and rotary shadowed with W-Ta. Note the continuity of the internal structure between body and tip and the presence of the inner sheath around the tip. (*B*) Tip of extended trichocyst, etched for 3 min at −105°C and rotary shadowed with W-Ta. Note the surface structure of the inner sheath and the internal structure of the tip (*arrows*) analogous to that of condensed trichocysts. (*C*) Poorly frozen, deep etched (6 min at −105°C) extended trichocyst. Note the highly perturbed morphology of the body structure and the well-preserved surface structure of the tip inner sheath. Bars: (*A* and *B*) 200 nm; (*C*) 400 nm.

a crystal from an apparently heterogeneous set of polypeptides? How is the precise shape of the crystal determined? By what mechanism can a protein crystal "expand" or "extend" to give a second crystal, quite different at least morphologically from the first one and with a different unit cell? What is the purpose of the extension and, more generally, what is the function of this exocytotic system? We cannot address all of these questions at present but harbor the conviction that they are related and that some understanding of this unusual edifice at the molecular level is necessary for an understanding of its properties at the organelle level, and of the role(s) that it may fulfill for the organism.

Small Protein Crystals

We have presented here the first x-ray diffraction patterns of *Paramecium* trichocysts and the first freeze-fracture and freeze-etch images of isolated trichocysts entirely compatible with the x-ray diffraction data, i.e., displaying periodicities in three dimensions. The number of relatively fine x-ray diffraction peaks given by unoriented specimens of condensed trichocysts and the fact that we can index these peaks on a monoclinic unit cell with dimensions correlated with those seen in the freeze-fracture electron microscope images, argue that trichocysts are indeed small protein crystals. That the diffraction is weak, that the peaks are larger than the di-

rect beam and that there is only continuous scattering beyond $s \sim(1/20)$ Å^{-1} indicate that these are not perfect crystals. While lattice disorder cannot be excluded, other factors that surely limit the diffraction are (*a*) the trichocyst matrix is so small (3 μm × 1 μm) that there are at most 100 unit cells aligned in any given direction, and (*b*) the polypeptides are heterogeneous so that different chemical species may occupy identical sites with respect to the symmetry of the crystal.

The unit cell dimensions found for the condensed trichocyst matrix (111 Å × 130 Å × 330 Å) could not have been predicted from the earlier ultrastructural studies. Only in the recent study of Peterson et al. (1987), which relied on similar freeze-fracture and freeze-etch techniques to those we have used, was an axial repeat of 310 Å reported. Fixed, embedded, and sectioned trichocysts as well as negatively stained trichocysts display periodic striations every 70–80 Å the length of the organelle, with an apparent repeat every two striations (140–160 Å). No consistent, distinct striations are evident in any other direction in images of stained trichocysts, with the exception of the complicated pattern of negatively stained trichocyst tips (Bannister, 1972; Hausmann et al., 1972). The axial repeat in the freeze-fracture images, corresponding to the unit cell dimension of 330 Å, is thus twice as large as the repeat in the images of stained trichocysts, and periodicities in the other directions are clearly visible. As mentioned in Results, there are some 60 monomers of 17-kD trichocyst protein per unit cell, so we expect there to be at least one intermediate level of packing, and the associated substructure may be visualized differently in images of stained trichocysts and in images of freeze-fractured and shadowed ones.

The differences between our images (and Fig. 7 of Peterson et al. [1987], which is similar to our Fig. 4 *A*) and those of fixed and stained trichocysts found in the literature may alternatively arise from perturbation of the structure. Fixation artifacts for trichocysts in whole cell preparations are well documented and led to a long-lived controversy as to whether "mature" as opposed to "juvenile" trichocysts retain a periodic structure or are amorphous (Yusa, 1963; Selman and Jurand, 1970; Bannister, 1972; Garofalo et al., 1983). In our hands, the structure of isolated trichocysts fixed with 0.1% glutaraldehyde according to a protocol that does not perturb crystals of fibrous proteins such as tropomyosin (White et al., 1987), is poorly preserved. The disorder is manifest in the x-ray diffraction patterns: the peaks are broadened or absent at *s* values greater than $\sim(1/80)$ Å^{-1}. In addition, much lower quality electron microscope images were obtained with trichocysts fixed in this way than with untreated ones (data not shown).

Extended trichocysts are, unlike the condensed form, amenable to negative staining, and a number of authors have reported a transverse period of 550–600 Å, which we have also found. Perhaps because of their high water content, extended trichocysts flatten on the grid and, especially if they are somewhat dilacerated after heating or dialysis (Steers et al., 1969; Hausmann et al., 1972; Pollack and Steers, 1973; Peterson et al., 1987), detailed patterns of fibrils may be seen. Hausmann et al. (1972; see also Fig. 7 in Hausmann, 1978) proposed a model for the extended trichocyst, largely on the basis of such images. The model in its over-all features is consistent with the data presented here. Layers of dense material are separated by 550 Å, the length of the trichocyst. The layers themselves are represented as agglomerations of spherical particles arranged in a square lattice (no dimensions are given). Thin filaments run between layers, at an angle of ~25° from the long axis of the trichocyst.

In the model of Hausmann et al. (1972), the axial repeat would be 2 × 550 Å since the interband regions, although identical, are rotated by 90° in consecutive layers. In most of our images, the true repeat appears to be every four bands (~2,300 Å). We note with amusement that we find the factor of 8 between the condensed and extended transverse periodicities expected by many authors (cf. Peterson et al., 1987) because of the global extension ratio of ~8. This is not required, and cannot be interpreted as meaning that a 111 × 130 × 330 Å condensed unit cell becomes by simple transformation a 115 × 115 × 2,300 Å extended unit cell: that would imply a roughly eightfold decrease in density, while the actual density decrease is only threefold.

The salient feature in images of stained trichocysts is the appearance of regularly spaced transverse bands of alternating electron dense and electron transparent material. In the freeze-fracture images, filaments are the salient feature, and they make complex patterns that give trichocysts the appearance of richly woven fabric (Figs. 4, *A* and *B*, and 6, *A* and *B*). The bands so characteristic of the earlier microscopy are replaced by regions, regularly spaced along the length of the condensed or extended trichocyst, in which filaments appear to be thickened, to be interrupted, or to cross each other. These differentiated regions probably reflect the complex interweaving of the series of filaments that traverse the trichocyst. We may add that in some images (see Figs. 4 *B* and 6 *B*), the filaments clearly appear tilted with respect to the trichocyst long axis and thereby inclined with respect to the elementary unit cell (cf. Fig. 8).

Secretory Vesicles with Crystalline Contents

Microcrystals of protein are not an unusual occurrence in cells. An example of a "functional" intracellular protein crystal that has been studied by x-ray diffraction is the parasporal inclusion of *Bacillus thuringiensis* (Holmes and Monro, 1965). In eucaryotic cells, crystalline inclusions are most often found in secretory or storage granules where proteins are sequestered and concentrated. Some well known examples are pancreatic β-granules which in many species contain insulin (but not proinsulin) in crystalline form (Howell and Tyhurst, 1982), cortical granules of animal oocytes which sometimes have "paracrystalline cores" (Guraya, 1982), and peroxisomes in which highly concentrated catabolic enzymes often form crystalline inclusions (deDuve, 1969). In these examples membrane-bound vesicles enclose high concentrations of proteins for transport and storage. The fact that these proteins may be present in crystalline form within the vesicle is not of primary importance, judging by the existence of species that do and do not contain the crystalline inclusions, but probably reflects the propensity of a given protein to crystallize at high concentration in the controlled medium provided by the vesicle (acid pH, for example). This remark can be turned around: the crystalline state is not necessary to achieve a concentration of 30%, the protein concentration in condensed trichocysts. Although secretory vesicles may enclose

protein crystals, they more often enclose comparably high concentrations of protein in an amorphous state, for example as charge-neutralized precipitates. We may thus ask why the contents of trichocysts (and other protozoan extrusosomes) are crystalline.

An important difference between trichocysts and metazoan secretory granules is their size. Metazoan secretory vesicles range in diameter from a few hundred angstroms to ~0.5 μm (Trifaró and Poisner, 1982). Trichocysts are thus some 10 times larger in their linear dimensions than the largest metazoan secretory granules, as are most protozoan extrusosomes (Hausmann, 1978). During exocytosis, at the moment when vesicular and plasma membranes fuse, vesicular contents must leave the vesicle rapidly. For small vesicles with soluble contents, this may be achieved by simple diffusion down a concentration gradient. For vesicles whose volume is at least 1,000 times greater, passive diffusion might be too slow. We suggest that this could be one reason why trichocyst contents are crystalline: protozoans solve the mechanical problem of emptying their huge secretory vesicles by designing their contents as rigid, compact structures that expand explosively upon contact with the extracellular medium so as to propel themselves out of the cell.

We gratefully acknowledge the expert advice and technical assistance of Jean-Claude Dedieu. We thank Daniel Taupin for the use of his automatic indexing program and the service of microdensitometry of the CNRS (Orsay) on whose computer the calculations were made. We thank Brigitte Krop for expert assistance with the x-ray experiments. We are particularly indebted to Janine Beisson for persistent support, encouragement and advice. We thank Jean Cohen and Vittorio Luzzati for their comments on the manuscript.

This work was supported in part by Contract Centre National de la Recherche Scientifique-Programme Interdisiplinaire de Recherche Scientifique et Médicale.

Received for publication 5 May 1987, and in revised form 25 June 1987.

References

Adoutte, A. 1987. Exocytosis: biogenesis, transport and secretion of trichocysts. *In* Paramecium. H.-D. Görtz, editor. Springer Verlag/Berlin. In press.

Adoutte, A., N. Garreau de Loubresse, and J. Beisson. 1984. Proteolytic cleavage and assembly of the crystalline secretion products of *Paramecium*. *J. Mol. Biol.* 180:1065–1081.

Adoutte, A., R. Ramanathan, R. M. Lewis, R. R. Dute, K.-Y. Ling, C. Kung, and D. L. Nelson. 1980. Biochemical studies of the excitable membrane of *Paramecium tetraurelia* III. Proteins of cilia and ciliary membranes. *J. Cell Biol.* 84:717–738.

Aggerbeck, L. P., and T. Gulik-Krzywicki. 1986. Studies of lipoproteins by freeze-fracture and etching electron microscopy. *Methods Enzymol.* 128: 457–472.

Anderer, R., and K. Hausmann. 1977. Properties and structure of isolated extrusive organelles. *J. Ultrastr. Res.* 60:21–26.

Bachmann, L., and W. W. Schmitt-Fumian. 1973. Spray-freezing and freeze-etching. *In* Freeze-Etching Techniques and Applications. E. L. Benedetti and P. Favard, editors. Société Française de Microscopie Electronique/Paris. 73–79.

Bannister, L. H. 1972. Structure of trichocysts in *Paramecium caudatum*. *J. Cell Sci.* 11:899–929.

Bilinski, M., H. Plattner, and H. Matt. 1981. Secretory protein decondensation as a distinct, Ca^{++} mediated event during the final steps of exocytosis in *Paramecium* cells. *J. Cell Biol.* 88:179–188.

Caspar, D. L. D., C. Cohen, and W. Longley. 1969. Tropomyosin: crystal structure, polymorphism and molecular interactions. *J. Mol. Biol.* 41: 87–107.

Cohen, C., and N. M. Tooney. 1974. Crystallization of a modified fibrinogen. *Nature (Lond.).* 251:659–660.

Cohen, C., D. L. D. Caspar, D. A. D. Parry, and R. M. Lucas. 1971. Tropomyosin crystal dynamics. *Cold Spring Harbor Symp. Quant. Biol.* 36: 205–216.

Cohen, J., and J. Beisson. 1980. Genetic analysis of the relationships between the cell surface and the nuclei in *Paramecium tetraurelia*. *Genetics.* 95: 797–818.

deDuve, C. 1969. Evolution of the peroxisome. *Ann. NY Acad. Sci.* 168:369–381.

Ehret, C. F., and G. De Haller. 1963. Origin, development and maturation of organelles and organelle systems of the cell surface in *Paramecium*. *J. Ultrastr. Res.* 6(Suppl.):3–41.

Garofalo, R. S., and B. H. Satir. 1984. *Paramecium* secretory granule content: quantitative studies on in vitro expansion and its regulation by calcium and pH. *J. Cell Biol.* 99:2193–2199.

Garofalo, R. S., D. M. Gilligan, and B. H. Satir. 1983. Calmodulin antagonists inhibit secretion in *Paramecium*. *J. Cell Biol.* 96:1072–1081.

Guraya, S. S. 1982. Recent progress in the structure, origin, composition, and function of cortical granules in animal egg. *Int. Rev. Cytol.* 78:257–360.

Hausmann, K. 1978. Extrusive organelles in protists. *Int. Rev. Cytol.* 52: 197–276.

Hausmann, K., W. Stockem, and K.-E. Wohlfarth-Bottererman. 1972. Cytologische Studien an Trichocysten I. Die Feinstruktur der gestreckten Spindeltrichocyste von *Paramecium caudatum*. *Cytobiologie.* 5:208–227.

Holmes, K. C., and R. E. Monro. 1965. Studies on the structure of parasporal inclusions from *Bacillus thuringiensis*. *J. Mol. Biol.* 14:572–581.

Howell, S. L., and M. Tyhurst. 1982. The insulin storage granule. *In* The Secretory Granule. A. M. Poisner, and J. M. Trifaro, editors. Elsevier Biomedical Press/Amsterdam. 155–172.

Koch, M. H. J., H. B. Stuhrmann, P. Vachette, and A. Tardieu. 1982. Small-angle X-ray scattering of solutions. *In* Uses of Synchotron Radiation in Biology. H. B. Stuhrmann, editor. Academic Press, Inc., New York. 223–253.

Matthews, B. W. 1968. Solvent content of protein crystals. *J. Mol. Biol.* 33:4911–497.

Matthews, B. W. 1985. Determination of protein molecular weight, hydration and packing from crystal density. *Methods Enzymol.* 114:176–187.

Mathews, F. S., and F. Lederer. 1976. Crystallographic study of baker's yeast cytochrome b2. *J. Mol. Biol.* 102:853–857.

Matt, H., H. Plattner, K. Reichel, M. Lefort-Tran, and J. Beisson. 1980. Genetic dissection of the final exocytosis steps in *Paramecium tetraurelia* cells: trigger analyses. *J. Cell Sci.* 46:41–60.

Palade, G. 1975. Intracellular aspects of the process of protein synthesis. *Science (Wash. DC).* 189:347–358.

Peterson, J. B., J. E. Heuser, and D. L. Nelson. 1987. Dissociation and reassociation of trichocyst proteins: biochemical and ultrastructural studies. *J. Cell Sci.* 87:3–25.

Poisner, A. M., and J. M. Trifaró. 1982. The Secretory Granule. Elsevier Biomedical Press/Amsterdam. pp. 415.

Pollock, S. 1974. Mutations affecting the trichocytes in *Paramecium aurelia* I. Morphology and description of the mutants. *J. Protozool.* 21:352–362.

Pollock, S., and E. Steers. 1973. Thermal solubilization of the trichocysts from *Paramecium aurelia*. *Exp. Cell Res.* 78:186–190.

Rauh, J. J., and D. L. Nelson. 1981. Calmodulin is a major component of extruded trichocysts from *Paramecium tetraurelia*. *J. Cell Biol.* 91:860–865.

Ruiz, F., A. Adoutte, M. Rossignol, and J. Beisson. 1976. Genetic analysis of morphogenetic processes in *Paramecium*. I. A mutation affecting trichocyst formation and nuclear division. *Genet. Res.* 27:109–122.

Sardet, C., A. Tardieu, and V. Luzzati. 1976. Shape and size of bovine rhodopsin: a small-angle X-ray scattering study of a rhodopsin-detergent complex. *J. Mol. Biol.* 105:383–407.

Schliwa, M., and J. Van Blerkom. 1981. Structural interactions of cytoskeletal components. *J. Cell Biol.* 90:222–235.

Selman, G. G., and A. Jurand. 1970. Trichocyst development during the fission cycle of *Paramecium aurelia*. *J. Gen. Microbiol.* 60:365–372.

Steers, E., J. Beisson, and J. T. Marchesi. 1969. A structural protein extracted from the trichocyst of *Paramecium aurelia*. *Exp. Cell Res.* 57:392–396.

Tartakoff, A. M. 1983. Perturbation of vesicular traffic with the carboxylic ionophore monensin. *Cell.* 32:1026–1028.

Taupin, D. 1968. Une méthode générale pour l'indexation de diagrammes de poudre. *J. Appl. Crystall.* 1:178–181.

Thomas, J. O., and R. D. Kornberg. 1975. An octamer of histone in chromatin and free in solution. *Proc. Natl. Acad. Sci. USA.* 72:2626–2630.

Tindall, S. 1986. Selection of chemical spacers to improve isoelectric focussing resolving power: implications for use in two-dimensional electrophoresis. *Anal. Biochem.* 159:287–294.

Tooney, N. M., and C. Cohen. 1977. Crystalline states of a modified fibrinogen. *J. Mol. Biol.* 110:363–385.

Trifaró, J. M., and A. M. Poisner. 1982. Common properties in the mechanisms of synthesis, processing and storage of secretory products. *In* The Secretory Granule. A. M. Poisner and J. M. Trifaro, editors. Elsevier Biomedical Press/Amsterdam. 387–407.

White, S. P., C. Cohen, and G. N. Phillips. 1987. Structure of the co-crystals of tropomyosin and troponin. *Nature (Lond.).* 325:826–828.

Xia, F., N. Shamala, P. H. Bethge, L. W. Lim, H. D. Bellamy, N. H. Xuong, F. Lederer, and F. S. Mathews. 1987. Three dimensional structure of flavocytochrome b_2 from baker's yeast at 3.0 A resolution. *Proc. Natl. Acad. Sci. USA.* 84:2629–2633.

Yusa, A. 1963. An electron microscopic study on regeneration of trichocysts in *Paramecium caudatum*. *J. Protozool.* 10:253–262.